GEOPHYSICAL RESEARCH LETTERS, VOL. 35, L23204, doi:10.1029/2008GL035790, 2008

Seasonally active frost-dust avalanches on a north polar scarp of Mars captured by HiRISE

Patrick Russell,[1] Nicolas Thomas,[1] Shane Byrne,[2] Kenneth Herkenhoff,[3] Kathryn Fishbaugh,[4] Nathan Bridges,[5] Chris Okubo,[3] Moses Milazzo,[3] Ingrid Daubar,[6] Candice Hansen,[5] and Alfred McEwen[6]

Received 25 August 2008; revised 23 October 2008; accepted 30 October 2008; published 6 December 2008.

[1] North-polar temporal monitoring by the High Resolution Imaging Science Experiment (HiRISE) orbiting Mars has discovered new, dramatic examples that Mars' CO_2-dominated seasonal volatile cycle is not limited to quiet deposition and sublimation of frost. In early northern martian spring, 2008, HiRISE captured several cases of CO_2 frost and dust cascading down a steep, polar scarp in discrete clouds. Analysis of morphology and process reveals these events to be similar to terrestrial powder avalanches, sluffs, and falls of loose, dry snow. Potential material sources and initiating mechanisms are discussed in the context of the Martian polar spring environment and of additional, active, aeolian processes observed on the plateau above the scarp. The scarp events are identified as a trigger for mass wasting of bright, fractured layers within the basal unit, and may indirectly influence the retreat rate of steep polar scarps in competing ways. **Citation:** Russell, P., et al. (2008), Seasonally active frost-dust avalanches on a north polar scarp of Mars captured by HiRISE, *Geophys. Res. Lett.*, *35*, L23204, doi:10.1029/2008GL035790.

1. Introduction

[2] The coming and going of snow cover on Earth is a loose analogy for the seasonal pattern of CO_2 frost cover on Mars. The behavior of CO_2 as the dominant component of an atmospheric system at temperatures and pressures not found on Earth is responsible for a host of small- and mid-scale seasonal processes and features on Mars that have not yet been fully explained. HiRISE [*McEwen et al.*, 2007], on NASA's Mars Reconnaissance Orbiter, has an image scale of ~0.30 m/pixel over a 6 km-wide surface swath with 3-band color along the center 1.2 km, making it particularly well suited to such investigations. The spacecraft's ability to point accurately off-nadir is also crucial to obtaining time-sequences of specific locations, essential to seasonal studies. During the early northern spring in February, 2008, HiRISE monitoring of frost-covered dunes fortuitously captured several billowing clouds of material in the progress of descending a steep polar scarp. These features represent an entirely new, dramatic class of seasonal processes whose role in Mars' volatile cycles is currently unknown.

[3] The opportunity to directly, visually investigate dynamic aspects of ongoing geological processes on another planet is rare. Here we describe these events, identify terrestrial analogs for some aspects, constrain the season of activity, compare them with additionally observed, active, particle-cloud features, estimate volumes of material and rates of movement, and explore their role in seasonal redistribution of material and net alteration of the polar scarp environment.

[4] The scarp in question, at 83.8°N, 235.5°E, is one of many cutting into the margins of the topographical dome of Planum Boreum (Figure S1 of the auxiliary material).[1] The upper ~500–700 m is H_2O ice-rich layers of the north polar layered deposits (NPLD) with varying dust content. Mars Orbiter Laser Altimeter data indicate maximum slopes of 60°–70° at this location over a baseline of ~300 m, and HiRISE imagery suggests that sections tens to ~100 m in height approach 90°. The lower, more gently sloping ~100–200 m is the stair-stepped expression of alternating resistant, bright, fractured layers and dark, sandy, weakly consolidated layers of the basal unit (BU) [*Herkenhoff et al.*, 2007, and references therein]. The relatively smooth, flat plain of the plateau at the top of the scarp is coated with the H_2O ice-rich residual cap, which itself becomes covered by the CO_2 ice-rich seasonal cap in winter.

2. Description

[5] Seven cloud features appear in 3 HiRISE images taken in the ~4 weeks spanning Ls 27°–39° (Figures 1, S1, and S2). We refer to the 7 clouds as examples 1a, 2a, 2b, 2c, 2d, 2e, and 3, according to the image in which they appear (1 = PSP_007140_2640 (Figure 1), 2 = PSP_007338_2640 (Figure 1), and 3 = PSP_007483_2640 (Figure S2)) and their position along the scarp from south to north. Two additional clouds, 1b and 1c, appear in the wider field-of-view MRO Context Camera (CTX) [*Malin et al.*, 2007] image co-aligned with PSP_007140_2640 (Figures 1 and S1). The sudden appearance of the cloud features in one image and their absence in prior and following images, as well as their limited, finite size, suggests that these are discrete, relatively short-lived events.

[1]Department of Space Research and Planetary Sciences, Physikalisches Institut, University of Bern, Bern, Switzerland.
[2]Lunar and Planetary Laboratory, University of Arizona, Tucson, Arizona, USA.
[3]U.S. Geological Survey, Flagstaff, Arizona, USA.
[4]Center for Earth and Planetary Studies, Smithsonian Air and Space Museum, Washington, D. C., USA.
[5]Jet Propulsion Lab, California Institute of Technology, Pasadena, California, USA.
[6]HiRISE Operations Center, Lunar and Planetary Laboratory, University of Arizona, Tucson, Arizona, USA.

0094-8276/08/2008GL035790$05.00

[1]Auxiliary materials are available in the HTML. doi:10.1029/2008GL035790.

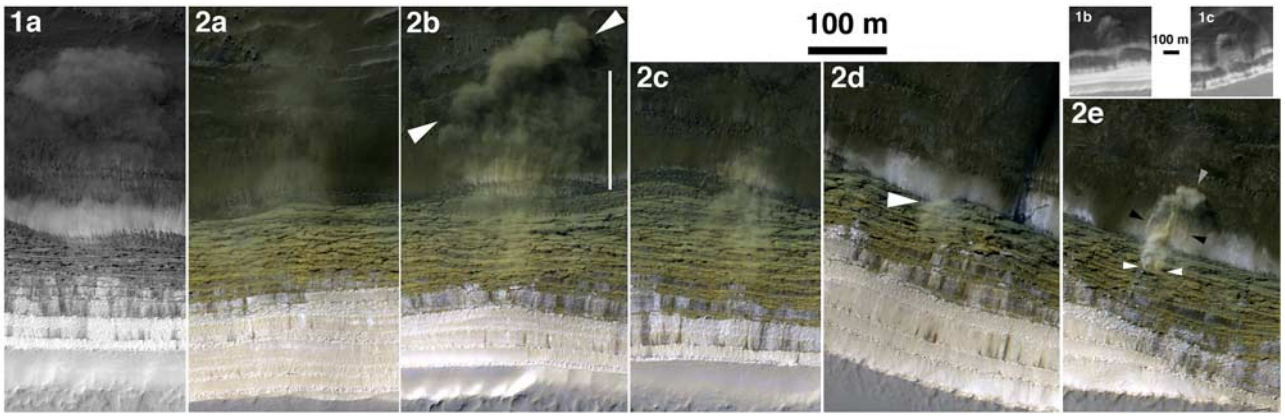

Figure 1. Cloud-forming events designated examples 1a–1c and 2a–2e, as labeled. Geographic context for all shown in Figure S1. Event 1a from HiIRSE PSP_007140_2640 (angle of incidence (i) = 73°, emission (e) = 7°, and Ls = 27°); events 1b and 1c from corresponding CTX P16_007140_2639_XI_83N125W_080203. Events 2a–2e from HiRISE PSP_007338_2640 (false color, i = 70°, e = 0.2°, Ls = 34°). Arrows in 2b, billowing front; line in 2b, roughly linear structure perpendicular to scarp. Arrow in 2d, likely highest concentration of cloud material above scarp base. In 2e, white arrows = discrete source on NPLD scarp; black arrows = small waves of material concentric to point of recent impact; grey arrow = incipient billowing front (~15–20 m high). Projection is with north to lower right, down-slope direction towards top, sun from upper left.

Observations of all 9 events contribute to our understanding of typical characteristics and variability of processes involved.

[6] Examples 2b and 2e contain the most visible internal structure of any events. In example 2b, the upslope boundary, located part way down the scarp just below the bright, white coatings of the upper layers, is thin and diffuse. The cloud closely follows the scarp face to its base and continues perpendicular to the scarp strike, hugging the BU surface. The cloud's downslope-most extent is a more dense, arcuate, billowing front ~200 m from the foot of the NPLD scarp. Based on shadow measurements, the height of the front is ~15–20 m. Behind the front, the cloud has a rough, lineated structure, and is probably <8 m thick, although shadows are difficult to discern over mottled terrain.

[7] Form and internal structural features suggest that cloud 2b is the trace of a path of descent along the scarp. The billowing front indicates the active movement of a relatively dense cloud through the ambient atmosphere. The rough, lineated section appears to be trailing or hanging behind the front. This section, and the general thinning of the cloud towards its diffuse, up-scarp boundary, is consistent with particles left lingering aloft by the recent passage of a coherent, moving concentration of particles.

[8] Evidence for all or parts of this morphology and behavior is also present in examples 1a–1c and 2c–2e, including arcuate, billowing, advancing fronts (examples 1a–1c), diffuse up-scarp margins just below the brightly coated NPLD layers (examples 1a–1c, 2c, and 2d), and remnant traces of ground-hugging paths on the BU leading away from the NPLD scarp (examples 1a–1c, and 2c–2e).

[9] The scarp-parallel cloud in example 2e is relatively high density, has a narrow, columnar form, and displays internal inhomogeneities, suggestive of particulate material actively cascading down a steep, irregular surface. From the point of encounter with the more gently sloping BU, a relatively concentrated stream of material extends perpendicularly away from the scarp. This stream leads to a higher, broader down-slope cloud which may be an incipient billowing front. Also associated with the encounter point are arc-shaped features that may be waves of material created as the high-density column impacts the BU surface and particles are deflected radially outwards. In conclusion, example 2e likely represents an earlier stage, during BU impact, relative to example 2b.

[10] Example 2d may have been captured just before impacting the BU, as the thickest cloud concentration within a relatively confined column is just above the scarp base. Thus, examples 2d, 2e, 2b, 1b, 1c, and 1a, respectively, can be fit into a sequence of successive stages of similar events.

[11] Example 2c is similar to the upslope-most portion of example 2b, but lack of continued downslope movement or a billowing front indicates that the amount of material involved may be insufficient for such developments. Example 2a is the thinnest, most diffuse cloud. While grossly similar in form to example 1a, example 2a likely reaches heights of 25 m (proximal to the scarp) to 50 m (distal to the scarp) above the BU surface. Example 2a, and perhaps 3, may represent the latest, dissipation stage of the above event sequence.

[12] Only in example 2e can a specific point of material-origin on the NPLD scarp be determined. In examples 1b–1c and 2b–2c, the back edge of the cloud on the scarp is less distinct (a bit more distinct in example 2d) but does not reach all the way to the top. In examples 1a, 2a, and 3, there is little to no evidence of the cloud on the scarp. In general, the relative abruptness of the upper edges of the clouds is roughly consistent with the sequence of stages outlined above.

3. Process

[13] The path and form of the cloud in most examples (1a–c, 2b, 2d–2e), suggest that the main concentration of particles moves on and along the surface (or just above it

over vertical sections) in early stages on the NPLD scarp, and moves with greater vertical distribution yet independently from and through the ambient atmosphere in later stages over the BU. Behavior and form thus differ distinctly from a thin, shapeless cloud moving high above, or minimally interacting with, the surface. In example 2e (and to a lesser extent 2d), cloud features and motion, especially the discrete source, narrow, collimated cloud, and NPLD scarp- and BU surface-interactions, are consistent with sediment-gravity flows, or mass wasting events, due primarily to the action of gravity directly on the particles (as opposed to being due to the primary motion of the fluid (i.e., the atmosphere) containing them, as in fluid-gravity flows or purely atmospheric entrainment events) [e.g., *Bloom*, 1998; *Hsü*, 2004]. Examples 1a–1c and 2b reflect later stages of such mass-wasting events. Example 2e reveals how momentum gained in descent of the scarp is both lost by impact and material deposition and transferred to downslope continuation of flow as a reduced-density cloud front. The persistence of particles lingering above the ground along the path of movement (both on the NPLD and BU), the billowing form and rising tendency of cloud fronts, and the increasingly diffuse source zone are consistent with separation of grains from the main, moving particle concentration by atmospheric drag. These stripped particles are entrained into suspension and become individually governed and maintained aloft by the dominance of atmospheric forces (e.g., related to Stokes settling and turbulence). Cloud appearance and behavior and particle-atmosphere interactions thus suggest that the best terrestrial mechanical analog for the particles involved is dry, loose snow or dust [*McClung and Schaerer*, 2006]. All this indicates the best specific analog for the large clouds currently moving over the BU with no visible, corresponding body of flowing material at their core to be a "powder avalanche" (1a–c, 2b); earlier, on-scarp stages may have involved higher concentrations of material flowing on the surface (currently the case in example 2e), as in "dry, loose snow avalanches", and the smaller events (2c, 2d) are similar to "sluffs", or falls of particles [*McClung and Schaerer*, 2006; *Voight et al.*, 1990; *Bloom*, 1998; *Cruden and Varnes*, 1996].

[14] Example 2a likely represents a post-mass wasting stage, in which particles disperse aloft and the cloud thins, fully in response to atmospheric forces. Alternatively, such thin clouds result when so little source material is initially involved that atmospheric drag forces are never collectively overcome by the kinetic energy of the falling particles, causing the grains to drift diffusely away from the scarp.

4. Composition and Source

[15] At this season, potential cloud constituents consistent with observed behavior are dust, H_2O ice/frost, and CO_2 ice/frost. HiRISE color of the clouds is more neutral than the dust-containing NPLD and redder than the bright, seasonal CO_2 frost at the top of the scarp. In example 2e, the plumes descending from the source location vary slightly in color. Both dust and frost are likely present. Furthermore, bright, white aprons at the NPLD-scarp base (Figure 1) are consistent in color, texture (some powdery or speckled), and location with concentrations of loose, frost-rich material that has cascaded down from the scarp, as is occurring in example 2e. Given the relative amounts of CO_2 and H_2O winter frost accumulation, the majority of the frost component is likely CO_2.

[16] All events are consistent with a scarp-face origin, although only in example 2e can this be confirmed. The accumulation of CO_2 on ledges and in crevices on the scarp may be directly from the atmosphere in winter, from higher on the scarp, and/or from the plateau above. The upper scarp is covered by bright, white CO_2 frost at the time these events are occurring (Figure 1). The up-scarp most trace of middle-stage event clouds (2b–d, 1b?, 1c) is just below these coated layers. During the period of event activity, streaks within this cover become more numerous and the minimum elevation of the cover rises (Figure S3a), consistent with shedding of CO_2 frost. The CO_2 cover is markedly less by Ls 50°. Thus, the timing of local CO_2 disappearance and cessation of event activity is also consistent with the upper-scarp frost cover being a source of event material. Several white marks tracing down from the CO_2 cover to the example 2e cloud origin may be further evidence of this source, or they may be aligned coincidentally. Plentiful CO_2 frost on the plateau may gradually accumulate on the scarp and eventually become incorporated into an event, but none of the events exhibit upslope continuity of their cloud material with the level of the plateau that would confirm a more direct provision of material.

[17] The seasonal dependence of the primary, CO_2 compositional component, of event activity, and of the source zone, adds to the analogy of these events as terrestrial dry, loose, H_2O snow processes in that the main compositional component is the solid form of the dominant volatile in the respective planet's seasonal cycle.

[18] We now examine whether there is any evidence for mass-wasting of H_2O-rich blocks from the NPLD scarp itself. Comparison of images before and during events reveals no missing blocks or sections of the fractured NPLD. Searches for the appearance of potentially fallen blocks or resolvable debris on the BU below the events yield only one candidate: a pair of ~2 m blocks ~145 m from the cliff base, following event 2b (Figure S4). There is no associated detritus or upslope trail of disturbance or deposition, except for an isolated disturbance in the ledge ~10 m upslope from the blocks. Appearance of these blocks is therefore most likely due to mass wasting of a fractured, ledge-forming, BU bright layer, as described by *Herkenhoff et al.* [2007] and *Russell et al.* [2008]. These blocks appear within a specific 29-day window, temporally and spatially coincident with an avalanche cloud. It is thus likely that the blocks, already at the verge of falling, were jarred loose by the avalanche event. This identifies a trigger for an important, recently discovered type of mass wasting within the BU. Without concurrent evidence for mass wasting of the host-scarp rock (H_2O ice), these events likely do not significantly alter the NPLD scarp itself and are not the type of rock falls or avalanches thought to contribute to accumulation of fan-shaped, H_2O-rich debris deposits on the BU [*Herkenhoff et al.*, 2007].

5. Discussion

[19] With the discovery of these frost-dust falls and avalanches, the HIRISE monitoring campaign was expanded

to ascertain 1) if they are seasonally limited, and 2) if they are a widely distributed phenomenon (Figure S5). No events are observed at the "discovery" scarp after Ls ~40°, at any of the other NPLD-BU scarps imaged this spring (all but 3 images are at Ls > 40°), or in the ~20 images of NPLD-BU scarps from the preceding northern summer (2006–2007). At the discovery scarp, events in 3 successive images and multiple, different events in two images suggest that activity is likely restricted to Ls ≤ ~40° and is frequent during this limited period. More robust determination of onset time, frequency, and geographic distribution requires dense monitoring of this and other scarps over at least Ls 0°–50°.

[20] Three potential triggers may destabilize fine, particulate material on the steep NPLD scarp. First, while the coincidence of 5 active events in one image might argue for an incident such as a marsquake or meteorite impact, the occurrence of events in 3 successive images over 4 weeks makes such a rare trigger highly unlikely. Instead, the restriction of these events to the season characterized by the rising of the spring sun and resultant CO_2 activity strongly favors a genetic relationship between CO_2 activity and the events. The expansion associated with the phase change of CO_2 sublimation at or near the surface of a CO_2 deposit is a more likely, second process. Finally, wind may destabilize scarp material. Relatively cold air moving across the plateau and sinking upon encountering warmer air above the scarp and plains may set up katabatic flow down the scarp face. Katabatic winds on Mars are likely strongest during the spring, especially when combined with sublimation flow [*Howard*, 2000]. Based on the abrupt beginning and short duration of events, the restriction of falling material to columns narrow relative to their spacing, and the clearly defined boundaries of many clouds, it is more likely intermittent or particularly strong, descending, katabatically-driven air gusts that occasionally cause disruption of fine scarp material (although non-katabatic, local turbulence below the plateau directly adjacent to the scarp face cannot be ruled out) than more idealized, broad-scale, uniform, sustained katabatic flow.

[21] The NPLD-scarp portions of clouds 1a–1c and 2b–2c are also consistent with material being entrained from the scarp face by descending atmospheric flow (as a fluid-gravity flow). If an air gust triggers destabilization and fall of material, it is certainly possible that the gust itself may also entrain some of the recently disturbed material; the resulting cloudy path would be hard to distinguish from the effects of ambient-atmosphere drag discussed above, and a continuum of processes may exist.

[22] Wind (including katabatic wind) also has the potential to provide material to, and hence cause, scarp events by entraining plateau-surface particles and delivering them to, and over, the plateau edge. Again, the form of the clouds would be more consistent with intermittent provision of material by gusts than by more broad, uniform, sustained flow. Wind-gust activity near the plateau edge is apparently confirmed by several particle-laden gusts caught in action at Ls 49.6° and 51.0° (Figures S6a and S6b). A contributory role for such particle gusts can only be ruled out explicitly for example 2e and possibly 2d. However, we observe neither particle gusts on the plateau nor cloudy material descending over the brightly coated scarp lip in any of the 3 images containing scarp events; the earliest event-stage observed is always on the scarp face.

[23] CTX imagery of the region captures two additional types of clouds that are distinctly different from the discrete events discussed hereto and are better ascribed to aeolian particle entrainment by more uniform, sustained, katabatic winds. The first type fringes and emanates from the plateau edge along a width of ~6.5 km, is diffuse, gradually thins towards its margins ~250–600 m away from the scarp lip, remains aloft at upper-scarp level, and has no associated descending columns, billowing fronts, or other structure (Figure S6c). It appears to persist over 4 images over ~12° Ls (Figure S5). The second type comprises individual and sets of jets of particulate material up to ~30 km long streaming along the NPLD surfaces to the south of the discovery scarp. These features are more similar to the sheets and jets of material emanating from SPLD surfaces on a yet larger scale observed by THEMIS [*Inada et al.*, 2007]. These jets occur in one of the images containing gusts, suggesting the latter may be a smaller manifestation of the former, possibly due to strong winds present over several days.

[24] That active particle-cloud features on or emanating from the plateau are directly observed yet are 1) distinctly different in form from scarp events, 2) not associated with or generating any scarp events, and 3) best explained by entrainment of plateau material by broader-scale, sustained wind activity, suggests that such wind activity is not responsible for the scarp events as well. It is also notable that the respective activity periods of plateau events and scarp events are mutually exclusive (Figure S5). The restriction of scarp events to early spring and their non-dependence on observed aeolian entrainment activity on the plateau (restricted to late spring) also supports a NPLD-scarp source for scarp-event material; the timing is consistent with frost and dust accumulation on the scarp over winter, destabilization and net material loss over early spring, and eventual disappearance of material from the scarp (including upper CO_2 cover) and accompanying cessation of event activity by mid spring. Meanwhile CO_2 remains plentiful on the plateau and the potential for, and observation of, katabatic winds and CO_2 entrainment continues.

[25] Monitoring of the fallen material at the NPLD-scarp base (Figure S3b) reveals the bright aprons mentioned above to be present through at least Ls 34°. Succeeding images reveal a gradually evolving, wavy pattern of bright and dark materials. Northern-summer images reveal the slopes here to consist of black, sandy BU material. Therefore, the scarp events do not lead to an ever-growing thickness of material but rather to temporary surface cover. Thus, the primary role of the scarp events is likely the seasonal redistribution of volatiles and dust. Direct implications for the long-term, directional evolution of steep polar scarps may therefore be minor, especially without concurrent evidence for mass-wasting of the NPLD scarp. However, HiRISE confirms that mass-wasting within the BU may be a major driver of steep scarp retreat [*Edgett et al.*, 2003; *Herkenhoff et al.*, 2007; *Russell et al.*, 2008]. Scarp events may indirectly affect such scarp retreat in two competing ways. First, the passage of powder avalanches disrupts previously fractured and under-cut bright layers of

the BU, as discussed above. Second, the temporary accumulation of deposits at the foot of the NPLD scarp may postpone the weathering and erosion of BU materials simply by covering them for much of the spring and summer.

[26] As a basis for comparison to other seasonal, CO_2-related processes, we estimate volumes of single events and seasonal totals. We also estimate rates of movement in a quantitative assessment of event dynamics. (Accompanying details are necessarily confined to Text S1). Using pixel locations of cloud front 2b in each of 3 individual images taken by 3, along-track aligned, color CCDs (essentially 3 frames in a movie-like sequence of the active event), the current speed of the advancing front is $\sim 2-6 \pm 2$ m/s (Text S1a). The speed attained by flowing granular material reaching the base of the NPLD scarp from a height of $\sim$300 m, as in example 2e, is estimated theoretically to be $\sim$40 m/s (Text S1b). Stoke's settling rate is $\sim$0.25 m/s (Text S1c). The persistence of cloud material trailing aloft behind advancing front 2b until the time of imaging may require a reasonable, net upwards contribution from atmospheric turbulence of up to $\sim$0.15 m/s. Although contrary to current observations, if an event were initiated by particulate material delivered over the scarp lip, then particles detached from the main concentration there would be able to settle $\sim 13-30$ m in the time before image acquisition, far short of the present location of the up-slope cloud margin in example 2b. An additional, average downwards component of 2–3 m/s would be required. The total volume of particles currently within the entire cloud 2b is equivalent to $\sim 10^2-10^3$ kg of CO_2/dust (Text S1d). Including material deposited in the bright, white apron at the foot of the NPLD scarp (using example 2e), all stages of one event may involve a total of $\sim 2 \times 10^3-2 \times 10^4$ kg of CO_2. In the observed activity season, there may be $\sim 30-320$ events per km of scarp, or $\sim 50-6000$ kg of CO_2 moved and deposited per m of scarp. The number of events per season that may be experienced at any given fixed location along the scarp ranges from 1–3 (min.) to 13–35 (max.).

6. Conclusions

[27] The nine active, steep-scarp events discovered by HiRISE are similar in behavior to terrestrial dry, loose snow avalanches, powder avalanches, sluffs, and falls of dry, loose snow. The material involved is mostly CO_2 ice/frost (with some dust) accumulated on and sourced from the NPLD scarp (including crevasses, ledges, and upper, frost-coated layers). While the plateau above may be a source of particles that slowly accumulate on the NPLD, there is not currently any evidence for a direct role of particulate plateau material in event initiation. Likely event triggers are sublimation-related gas expansion on the scarp and wind gusts on the scarp face (from katabatic, sublimation, and/or local turbulent flow). Additional, active particle clouds observed near this scarp represent atmospheric entrainment processes distinctly different from the falls and avalanches, likely resulting from broader-scale, more sustained, possibly katabatic winds. None of these additional clouds are observed to contribute to avalanche and fall events, and the respective periods of activity are exclusive of each other. Avalanche events occasionally trigger mass wasting of fractured layers within the BU. While this may hasten steep scarp retreat, the deposition of a seasonal cover at the base of the NPLD may have the opposite effect.

[28] **Acknowledgments.** Thank you to P. Thomas and M. Koutnik for helpful reviews, the HiRISE and HiROC teams for help and discussions, and Sarah Mattson for jitter analysis. This work was supported in part by the Swiss National Science Foundation.

References

Bloom, A. (1998), *Geomorphology: A Systematic Analysis of Late Cenozoic Landforms*, 3rd ed., Prentice-Hall, Upper Saddle River, N. J.

Cruden, D., and D. Varnes (1996), Landslide types and processes, in *Landslides: Investigation and Mitigation*, *Spec. Rep. Natl. Res. Counc. U.S. Transp. Res. Board*, vol. 247, edited by A. Turner and R. Schuster, pp. 36–75, Natl. Acad. Press, Washington, D. C.

Edgett, K., R. Williams, M. Malin, B. Cantor, and P. Thomas (2003), Mars landscape evolution: Influence of stratigraphy on geomorphology in the north polar region, *Geomorphology*, *52*, 289–297.

Herkenhoff, K., S. Byrne, P. Russell, K. Fishbaugh, and A. McEwen (2007), Meter-scale morphology of the north polar region of Mars, *Science*, *317*, 1711–1715, doi:10.1126/science.1143544.

Howard, A. (2000), The role of eolian processes in forming surface features of the Martian polar layered deposits, *Icarus*, *144*, 267–288, doi:10.1006/icar.1999.6305.

Hsü, K. J. (2004), *Physics of Sedimentology: Textbook and Reference*, 2nd ed., Springer, Berlin.

Inada, A., M. Richardson, T. McConnochie, M. Strausberg, H. Wang, and J. Bell (2007), High-resolution atmospheric observations by the Mars Odyssey Thermal Emission Imaging System, *Icarus*, *192*, 378–395, doi:10.1016/j.icarus.2007.07.020.

Malin, M. C., et al. (2007), Context Camera investigation on board the Mars Reconnaissance Orbiter, *J. Geophys. Res.*, *112*, E05S04, doi:10.1029/2006JE002808.

McClung, D., and P. A. Schaerer (2006), *The Avalanche Handbook*, 3rd ed., Mountaineers, Seattle, Wash.

McEwen, A. S., et al. (2007), Mars Reconnaissance Orbiter's High Resolution Imaging Science Experiment (HiRISE), *J. Geophys. Res.*, *112*, E05S02, doi:10.1029/2005JE002605.

Russell, P., S. Byrne, K. Herkenhoff, K. Fishbaugh, N. Thomas, and A. McEwen (2008), Active mass-wasting processes on Mars' north polar scarps discovered by HiRISE, *Lunar Planet. Sci.*, *XXXIX*, Abstract 2313.

Voight, B., B. Armstrong, R. Armstrong, D. Bowles, R. Brown, S. Ferguson, J. Fredston, J. Kiusalaas, R. McFarlane, and R. Pennimman (1990), *Snow Avalanche Hazards and Mitigation in the United States*, Natl. Acad. Press, Washington, D. C.

N. Bridges and C. Hansen, Jet Propulsion Lab, California Institute of Technology, 4800 Oak Grove Drive, Pasadena, CA 91109, USA. (nathan.t.bridges@jpl.nasa.gov; candice.j.hansen@jpl.nasa.gov)

S. Byrne, Lunar and Planetary Laboratory, University of Arizona, 1629 E. University Boulevard, Tucson, AZ 85721, USA. (shane@lpl.arizona.edu)

I. Daubar and A. McEwen, HiRISE Operations Center, Lunar and Planetary Laboratory, University of Arizona, 1541 E. University Boulevard, Tucson, AZ 85721, USA. (ingrid@pirl.lpl.arizona.edu; mcewen@pirl.lpl.arizona.edu)

K. Fishbaugh, Center for Earth and Planetary Studies, Smithsonian Air and Space Museum, 601 Independence Avenue SW, Washington, DC 20024, USA. (fishbaughke@si.edu)

K. Herkenhoff, M. Milazzo, and C. Okubo, Astrogeology Team, U.S. Geological Survey, 2255 N. Gemini Drive, Flagstaff, AZ 86001, USA. (kherkenhoff@usgs.gov; moses@usgs.gov; cokubo@usgs.gov)

P. Russell and N. Thomas, Department of Space Research and Planetary Sciences, Physikalisches Institut, University of Bern, Sidlerstrasse 5, CH-3012 Bern, Switzerland. (patrick.russell@space.unibe.ch; nicolas.thomas@space.unibe.ch)